Journal of Field Robotics

WILEY

RESEARCH ARTICLE OPEN ACCESS

Developing a Climbing Robot for Stay Cable Maintenance With Security and Rescue Mechanisms

Zhenliang Zheng[1,2] | Chao Wang[2] | Xiaoli Hu[2] | Lun Zhang[2] | Wenchao Zhang[2] | Yongyuan Xu[1,3] | Pengfei Liu[2] | Xufang Pang[2] | Tin Lun Lam[1,2] | Ning Ding[2]

[1]School of Science and Engineering, The Chinese University of Hong Kong (CUHK), Shenzhen, China | [2]Shenzhen Institute of Artificial Intelligence and Robotics for Society (AIRS), Shenzhen, China | [3]Institute of Control Systems, Hamburg University of Technology, Hamburg, Germany

Correspondence: Tin Lun Lam (tllam@cuhk.edu.cn) | Ning Ding (dingning@cuhk.edu.cn)

Received: 30 August 2024 | **Revised:** 9 December 2024 | **Accepted:** 2 January 2025

Funding: This study was funded by Shenzhen Science and Technology Innovation Council (grant GJHZ20240218114202004), Shenzhen Science and Technology Program (grants 20220817171811004, JSGG20210802152801004), the National Natural Science Foundation of China (grant 62106155), the Guangdong Basic and Applied Basic Research Foundation (grants 2023A1515012570, 2021B1515420005), the Shenzhen Major Science Technology Project (grant KJZD20230923114810022), and the Longgang District Shenzhen's "Ten Action Plan" for Supporting Innovation Projects (grant LGKCSDPT2024002).

Keywords: cable maintenance | climbing robot | field application | rescue robot | security and rescue mechanisms

ABSTRACT

The significance of climbing robotic systems for cable maintenance is escalating in both academic research and real-world applications. As these systems are poised for real-world deployment, it is imperative to develop security and rescue mechanisms that ensure robots' intrinsic safety and robustness in dealing with uncertainty factors. This study presents a novel cable climbing robot designed with a climbing platform, a robotic manipulator integrated with specialized maintenance tools, and a gripper to withstand dynamic loads and impacts from maintenance operations. In addition, we propose the variable-damping safe-landing mechanism, the rescue mechanism, and the fusible gripper mechanism to counteract substantial disturbances in worst-case scenarios. Extensive experiments have been conducted to evaluate the proposed robot and its security and rescue mechanisms. The cable climbing robot has a heavy-duty capacity of 45 kg and an obstacle-negotiation ability of 10 mm. It also demonstrated its capabilities in various maintenance tasks, such as cable inspection, grinding, or repair. The variable-damping safe-landing mechanism was tested, showing the maximum falling speed can decrease from 1 to 0.1 m/s to promise safety, and the falling time can increase from about 5 to 45 s. Meanwhile, the rescue mechanism successfully retrieved the trapped robot. The results demonstrate the capabilities of the cable climbing robot and the feasibility of using the security and rescue mechanisms for the climbing robotic system, which have implications that the cable climbing robot with security and rescue mechanisms is more reliable and can be deployed in the real world with greater confidence.

1 | Introduction

Long-span cable-stayed bridges, such as the Hong Kong-Zhuhai-Macau Bridge, are often constructed in challenging and exposed environments, spanning ravines, mountains, valleys, lakes, rivers, seas, and urban structures. These bridges play a crucial role in facilitating efficient communication and transportation in modern society. However, the bridge cables, the primary components of cable-stayed bridges, are susceptible to various forms of deterioration due to factors such as temperature fluctuations, mechanical loading, corrosion of strand bundles, fire hazards related to high-density polyethylene sheathing, freeze-thaw cycles, exposure to airborne chlorides in marine settings, and the presence of chlorides in de-icing salts. The increased frequency of traffic and the occurrence of extreme weather conditions impose additional stresses on these

cables, leading to potential safety hazards. Regular inspections are essential to identify cable defects and deterioration points and ensure the structural integrity and safety of the bridge. Surveys conducted in Europe and North America have revealed significant degradation in a large proportion of existing bridge cables, necessitating prompt repair and maintenance interventions (Sika 2021).

Cable climbing robotic systems have the potential to revolutionize this field, from cable inspection to cable repair, for example, a cable climbing robot carries high-definition cameras or a magnetic flux leakage (MFL) sensor (whose weight is more than 20 kg) to detect any imperfections along a cable surface or to identify section loss and the corrosion of steel strands inside a cable or a cable climbing robot carries specialized maintenance tools for cable cleaning, cable repairing, or cable grinding. Cable climbing robots are envisioned to play an essential role in maintenance activities.

Despite a promising future, researchers need to consider some crucial aspects that are underexplored or neglected in realistic deployments. One of the main reasons cable climbing robots have not been widely adopted in real-world applications is that there is no consensus on designing robotic systems that include security and rescue mechanisms. The lack of security and rescue mechanisms in the cable maintenance field hinders this robotic technology's adoption.

1.1 | State of the Art

Various types of cable climbing robots have been developed to climb bridge cables. A pneumatic worming climbing mechanism by Luo et al. (2007) was also developed for cable painting and rust-detecting by Luo et al. while the dry weight of the robotic system was 160 kg. Li et al. (2009) designed a continuous climbing pneumatic cable maintenance robot that is used to paint cables automatically; the prototype was made out and tested only in the laboratory. Yuan et al. (2010) developed a cable maintenance robot; the robot can automatically perform nondestructive testing, cleaning, painting, and other maintenance work for cable-stayed bridge cables with any inclination angle. However, the climbing substrate is required as a magnetic adsorption material. Tavakoli et al. developed a climbing robot—3DCLIMBER (Tavakoli et al. 2011, 2012), which can travel along a pole or tubular structure with bends and branches. Xu, Wang, and Cao (2011) Xu, Wang, and Wang (2011) developed several bilateral/trilateral wheel-based cable inspection robots. They also proposed a cable climbing robot based on a quadrilateral independent suspension that can automatically repair the deterioration points of the cable surfaces with grinding, cleaning, spray coating, and winding mechanisms according to the surface damage encountered by Xu et al. (2021). MRC ^{2}IN-II (Cho et al. 2013b, 2016) is one of the cable climbing robots designed for cable inspection by Cho et al. The robot has caterpillar tracks instead of wheels, and thus, the robot can move smoothly on the bumpy surface of the cable, and it has been applied successfully on the Yeong-Jong Grand Bridge. Infraspect Engineering Company IPC (2015) has released several cable inspection robots, one of the most successful commercialized robotic crawlers. They can transfer high-definition video and Magnetic Flux Leakage (MFL) information to the base station. Our team also developed five generations of cable climbing robots—CCRobot series (Zheng et al. 2018; Zheng and Ding 2019; Ding et al. 2020; Zhang et al. 2021; Zheng et al. 2021, 2022), aimed to enhance the climbing speed and load capacity simultaneously in an autonomous climbing single machine. CCRobot-I and CCRobot-II (Zheng et al. 2018; Zheng and Ding 2019) adopt palm-based extension-compression climbing gait and alternating-sliding climbing gait, respectively, which are bio-inspired by the inchworm and monkey in nature, to increase the payload capacity. CCRobot-III, and CCRobot-IV (Ding et al. 2020; Zhang et al. 2021; Zheng et al. 2021) use the split-type cable-driven approach to lengthen the step stroke, CCRobot-IV (Zhang et al. 2021; Zheng et al. 2021) integrated a new quad-ducted propeller-driven precursor into the CCRobot-III (Ding et al. 2020) design to enhance the climbing efficiency further. A more exotic approach was presented in CCRobot-V (Zheng et al. 2022), which employed a cooperative multi-robot system and provided a mobile work line for superlong bridge cable inspection and maintenance.

To the best of the authors' knowledge, there is little related research in the literature about designing robotic systems that include security and rescue mechanisms. Xu, Wang, and Cao (2011) and Xu, Wang, and Wang (2011) developed a novel safety landing mechanism for a cable inspection robot. This design can enable the robot to land at a controllable velocity in case of power shortages or electrical malfunctions. Cho et al. (2016) designed a clutch mechanism and a safe landing mechanism to let the robot climb down and control the robot's movement through a disk damper. A fault-tolerant control system or a backup battery is needed to activate the clutch mechanism. Our team (Zheng et al. 2018; Zheng and Ding 2019; Ding et al. 2020; Zhang et al. 2021; Zheng et al. 2021, 2022) utilizes palm-based extension-compression climbing gait (Zheng et al. 2018) or alternating-sliding climbing gaits (Zheng and Ding 2019) or a split-type climbing gaits (Ding et al. 2020; Zhang et al. 2021; Zheng et al. 2021, 2022) to ensure at least one pair of palms keeps clamping on the stay cable, preventing the robot slips down along the stay cable. However, these robotic teams had not considered how to retrieve the robots trapped on the upper-air stay cable. Besides, we have not searched for other robotic solutions that pay attention to robots' intrinsic safety and robustness.

1.2 | Motivation

As can be observed from Table 1, most of the proposed robots that are reported in the literature are designed for cable inspection (Xu, Wang, and Wang 2011; Tavakoli et al. 2012, 2011; Cho, Jin, et al. 2013; Cho, Kim, et al. 2013, Cho et al. 2014; IPC 2015; Cho et al. 2016; Wang et al. 2021; Nguyen et al. 2022; Nguyen et al. 2024) with carrying detection sensors, and only a small amount of cable climbing robots are used for cable maintenance, including stay cable cleaning, repairing, coating, and grinding (Luo et al. 2007; Li et al. 2009; Yuan et al. 2010; Xu et al. 2021). Since inspection tasks only need to move robots with low loads, while maintenance tasks always need to equip one or dual six/seven Degree of Freedom (DoF) robotic manipulator or

TABLE 1 | Performance comparison.

	Implementation	Weight (kg)	Payload (kg)	Obstacle-Crossing Capacity (mm)	Security Mechanisms	Rescue Mechanisms
CMR, Luo et al. (2007)	Painting	160	140	N/A	×	×
PCMR, Li et al. (2009)	Cleaning; Painting	75	N/A	N/A	×	×
RCMR, Yuan et al. (2010)	Cleaning; Spraying	80	150	N/A	×	×
3DClimber, Tavakoli et al. (2011)	Inspection	42	1	N/A	×	×
MRC ^{2}IN-I, Cho et al. (2013b)	Inspection	30	9	3.9	×	×
MRC ^{2}IN-II, Cho et al. (2016)	Inspection	30	N/A	5	✓	×
Bilateral Robot 1, Xu, Wang, and Cao (2011)	Inspection	5	4	≤ 5	×	×
Bilateral Robot 2, Xu et al. (2014)	Inspection	4	1.5	≤ 5	×	×
Trilateral Robot, Xu, Hu, and Jiang (2015)	Inspection	N/A	3.2	5.6	×	×
3DClimber, Tavakoli et al. (2011)	Inspection	42	1	N/A	×	×
Treebot, Lam and Xu (2011)	Inspection	0.6	1.75	N/A	×	×
CCRobot-I, Zheng, Hu, and Ding (2018)	Internal inspection	15	30	12	✓	×
CCRobot-II, Zheng and Ding (2019)	Internal inspection	25	30	15	✓	×
CCRobot-III, Ding et al. (2020)	Internal inspection	28.3	40	5	✓	×
This Study	Grinding; repair	25	45	10	✓	✓

maintenance tools or specialized end effectors, including grinding head, milling head, hot melt gun, coating gun, cleaning head, winding device, and so on. Typically, a six/seven DoF robotic manipulator and a specialized tool or end effector weigh more than 20 kg. Current cable climbing robots can rarely directly equip such combination units due to their low load capacity.

Additionally, despite some available cable climbing systems that have been applied in laboratory and field environments, robotic climbing solutions that pay attention to robots' intrinsic safety and robustness are rare. In fact, when cable climbing robots are deployed in the real world, numerous uncertainty factors and disturbances emerge in this process, posing considerable dangers or damage. Our team has developed five generations of cable climbing robots—CCRobot series (Zheng et al. 2018; Zheng and Ding 2019; Ding et al. 2020; Zhang et al. 2021; Zheng et al. 2021, 2022) and have deployed these robotic systems in-situ for practical application, to this end, we can conclude three kinds of potential uncertainty factors and security risk:

- First, the wheel-based cable climbing robot may fall from a height of hundreds of meters along the stay cable due to a defect or loss of power. In this case, the cable climbing robot would keep speeding up by its own weight with constant acceleration until crashing on the ground, causing serious damage to the robot and potential security risks.
- Another phenomenon is the robot being trapped or stuck on the upper-air stay cable and can not return to the ground due to a fault, such as a pit or a step. In this case, we have to use cranes, bucket trucks, hydraulic lifts, or hanging brackets to carry workers to the upper-air stay cable to retrieve the trapped robot, which is inefficient and unsafe.
- A more delicate matter is the releasing of the palm/gripper for palm/gripper-based climbing robots (Lam and Xu 2012b, 2011, 2012a, 2013; Zheng et al. 2018; Zheng and Ding 2019; Ding et al. 2020; Zhang et al. 2021; Zheng et al. 2021, 2022; Parness et al. 2013; Tavakoli et al. 2012; Spenko et al. 2008; Backus et al. 2020; Hong et al. 2022). Learning from our precious publications of tree-climbing robots (Treebot series) (Lam and Xu 2012b, 2011, 2012a, 2013) and cable-climbing robots (CCRobot series) (Zheng et al. 2018; Zheng and Ding 2019; Ding et al. 2020; Zhang et al. 2021; Zheng et al. 2021, 2022), the gripper is designed to anchor on the tree or stay cable to withstand and overcome dynamic loads and impacts introduced by environment disturbances, such as wind load or maintenance operation such as cable grinding, milling, or repair. When the gripper keeps on the anchor status and can not open the gripper due to mechanical breakdown, control fault, or power down, retrieving the robot is a formidable challenge.

Consequently, the attainment of intrinsic safety and robustness characteristics in an anti-gravity environment poses excellent significance for a cable climbing robotic system. It is an urgent issue that needs to be settled for robotics practical application.

Analyzing the state-of-the-art cable climbing robots reveals that the existing solutions can not possess maintenance capacity with heavy load characteristics. Most cable climbing robots neglect their security and rescue mechanism design and can not be deployed in the real world. As a result, to facilitate the practical deployment and widespread adoption of the robotic system in the real world, it is imperative to develop cable climbing robots that combine the advantages of heavy load, intrinsic safety, and robustness and reliability.

1.3 | Contribution

In this study, we developed a novel climbing robot for stay cable maintenance, as shown in Figure 1. This system comprises a moving platform, which could integrate a robotic manipulator or specialized inspection and maintenance tools, and a cable rescue robot, which can capture the moving platform and drag it back to the ground. The moving platform is equipped with a customized griper.

The contribution of this paper is manifold and can be summarized as follows:

- A novel climbing robot platform for stay cable maintenance is introduced. It combines the advantages of heavy load, intrinsic safety, and robustness, increases reliability, and contributes to confidence enhancement in field deployment, advancing state-of-the-art climbing technology. It holds promise for future robotics practical applications in stay cable maintenance.
- Several pioneering security and rescue mechanisms for cable climbing robots have been introduced. The proposed methodology establishes a climbing design paradigm to consider the intrinsic safety and robustness of climbing robots for deployment in the real world under scenarios with challenging gravity-adversarial conditions, opening

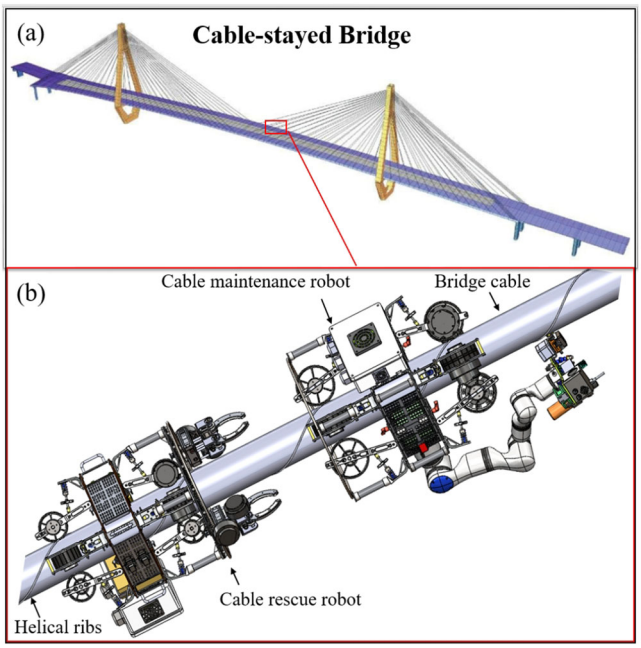

FIGURE 1 | (a) Schematic diagram of a cable-stayed bridge. (b) The overall design of the climbing robot for stay cable maintenance with security and rescue mechanisms. [Color figure can be viewed at wileyonlinelibrary.com]

the opportunity and paving the way for developing high-quality climbing robots. Researchers can leverage this approach as a foundation for designing climbing systems in diverse applications.

- Extensive experiments have been conducted to assess the effectiveness of the proposed robot and the security and rescue mechanisms. The results presented in this work demonstrate the capabilities of the cable climbing robot and the feasibility of using the security and rescue mechanisms for the climbing robotic system, which has implications that the cable climbing robot with security and rescue mechanisms is more reliable and can be deployed in the real world with greater confidence.

1.4 | Structure of the Paper

The structure of the remaining sections in this paper is outlined as follows. Section 2 will first address the system design of the cable climbing robots, including the cable maintenance robot and the cable rescue robot, elaborated by an in-depth exploration of the mechanical design. Its security and rescue mechanisms are presented in Section 3, and the model and the obstacle-negotiation capacity of the cable climbing robot are analyzed and formulated in Section 4. The admissible workspace of the capturing grippers for the capturing region is identified and analyzed comprehensively, and the control system is presented in Section 5. Section 6 describes and presents the prototype and experiments. Finally, conclusions and future works are drawn in Section 7.

2 | Robot System Design

As illustrated in Figure 1, the climbing robot system comprises a cable maintenance robot and a cable rescue robot. Generally, the cable maintenance robot is used for cable maintenance operations, while the cable rescue robot is only used in this condition when the cable maintenance robot is trapped on the upper-air cable. In that case, we need to assign the cable rescue robot to drag the trapped robot back to the ground.

2.1 | Cable Maintenance Robot Design

Cable maintenance robot is the main robot in the robot system. Unlike the conventional simplified cable maintenance robot, this cable maintenance robot possesses the heavy-duty ability to integrate a robotic manipulator and a specialized tools unit. Figure 2 shows the cable maintenance robot's proposed computer-aided design (CAD) model. It comprises a climbing platform, a robotic manipulator, a specialized tools unit, a gripper, a control cabinet, and a capturing rod. The total weight of the robot is approximately 25 kg.

1. The climbing platform incorporates eight locomotion and adhesion units and a robot frame. Four locomotion and adhesion units are uniformly distributed around the upper part of the robot frame, and the other four are mounted on the lower part. An EC servo motor wheel drives the unit with a radius of 50 mm. The wheel clamps down on the bridge cable by a four-bar linkage suspension mechanism using pre-compressed tension springs for adhesion. We can control the pressure between the wheels and cable surfaces by adjusting the length of the adjustable linkage, as shown in Figure 3. The modular independent design method makes every locomotion and adhesion unit independent of others, improving the stable climbing ability and the capacity to surmount obstacles.
2. The gripper is mounted in the robot frame. The gripping module's design follows the CCRobot series style that we have developed in Zheng, Hu, and Ding (2018), Zheng and Ding (2019), Ding et al. (2020). The kinematical transmission and the appearance are consistent and unitive, aiming at maximizing power delivery and maintaining

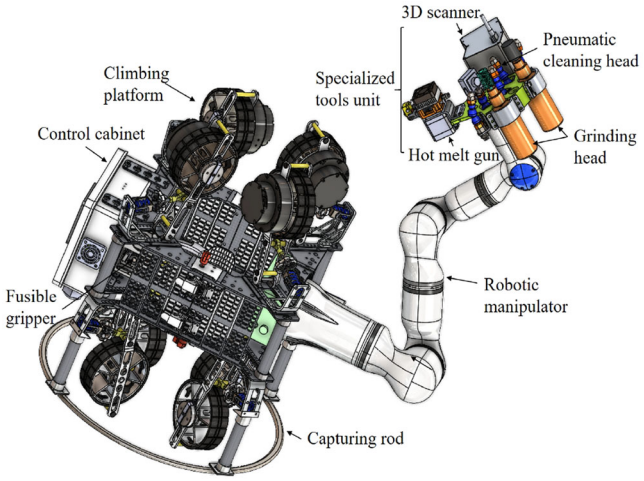

FIGURE 2 | Structure of the cable maintenance robot, which integrates with a robotic manipulator and specialized tools. [Color figure can be viewed at wileyonlinelibrary.com]

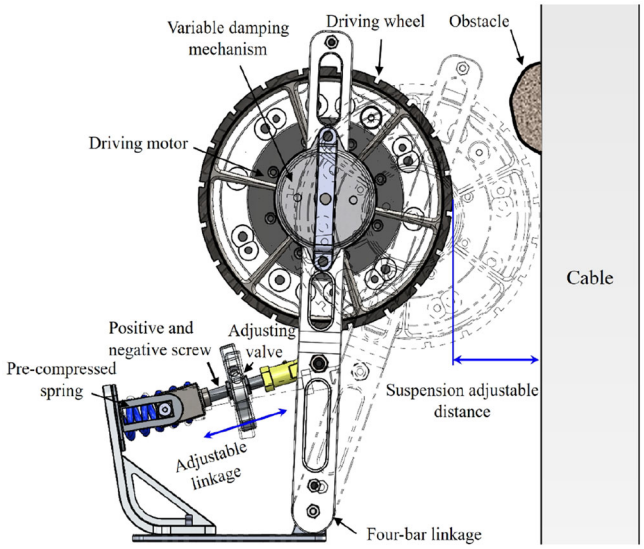

FIGURE 3 | The locomotion and adhesion unit, in which a positive and negative screw is used to adjust the length of the linkage leading to the changing of the distance between the driving wheel and the cable surface. [Color figure can be viewed at wileyonlinelibrary.com]

energy conservation when the robot prepares to do maintenance operations, such as cable grinding, cleaning, or repair. The gripper anchors to the stay cable surface to withstand and overcome dynamic loads and impacts introduced by contact forces and torques or environmental disturbances, offering a stable working condition for the cable maintenance robot.

3. A 7-DoF robotic manipulator has been chosen for the maintenance tasks on the stay cable due to its enhanced flexibility and reachability, particularly toward the rear Section of the stay cable.
4. The specialized tool unit consists of a grinding head, a hot melt gun, a pneumatic cleaning gun, a vision sensor, and a laser 3D scanner.

2.2 | Cable Rescue Robot Design

The **Cable rescue robot** is a wheel-based cable climbing robot. It comprises a climbing platform, circular rail, control cabinet, and capturing grippers. Figure 4 shows the cable rescue robot's proposed CAD model. The structure of the climbing platform is analogous to the precursor of CCRobot-V (Zheng et al. 2022) and the cable maintenance robot, as aforementioned, both equipped with locomotion and adhesion units. Two capturing grippers with sliders are symmetrically mounted on the circular rail, which is used to adjust the positions of the capturing grippers to grasp the capture rod. EC servo motors drive them, and every motor integrates a planetary gear.

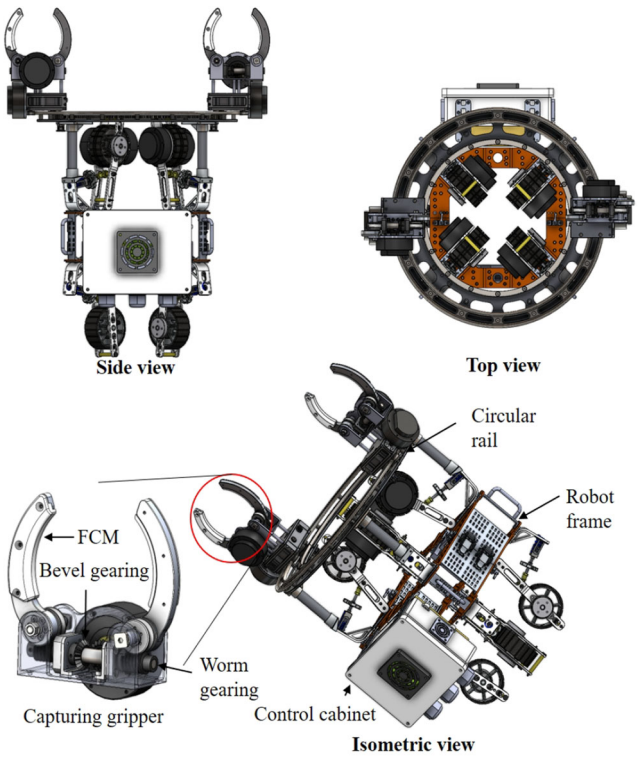

FIGURE 4 | Structure of the cable rescue robot, which integrates with a circular rail and two capturing grippers. [Color figure can be viewed at wileyonlinelibrary.com]

Besides, the capturing gripper is customized; a flexible covering material (FCM) is covered on the gripper legs to enhance the frictional interaction between the gripping module and the capturing rod on the cable maintenance robot. A three-stage transmission is employed to transmit substantial force and torque, with worm gearing utilized in the final stage. The self-locking nature of worm gearing ensures that the gripping module joints are non-back drivable, enabling the gripper to maintain joint poses when the cable rescue robot drags the cable maintenance robot toward the ground along the stay cable.

2.3 | Installation Design

Both the cable maintenance robot and the cable rescue robot are based on the same climbing platform, so in this part, we focus on the installation of the climbing platform. Figure 5 shows its process. The climbing platform consists of two nearly symmetrical components. A hinge-and-buckle structure is adopted to open and close the climbing platform in the middle (see Figure 5a), which makes the installation process more convenient. During the installation process 5a, the grippers must remain open to prevent collisions between the palms and the cable surface. Before installing the robot on the stay cable, the linkage in every locomotion and adhesion unit is adjusted to the shortest length (see Figure 3), causing the driving wheel to spread out. This design helps avoid confronting the tension when the climbing platform is snapped around the stay cable. A small gap between the stay cable surface and the driving wheel, as shown in Figure 5b, allows the robot to slide on the stay cable. Then, by increasing the length of the linkage in every locomotion and adhesion unit (see Figure 3) through the employment of the positive and negative screw, the driving wheel moves toward the stay cable, exerting appropriate pressure on the stay cable (see Figure 5c); since the clamping force is distributed on the eight locomotion and adhesion units, the needed clamp force for every locomotion and adhesion unit would not be very big, and a specialized adhesion tool for clamping is not required for the installation process.

3 | Security and Rescue Mechanisms

This Section presents the security and rescue mechanisms for the climbing robots in detail based on the robot system design. In this study, the security and rescue mechanisms mainly include a variable-damping safe-landing mechanism, a robotic rescue mechanism, and a fusible gripper mechanism.

3.1 | Variable-Damping Safe-Landing Mechanism

Owing to the advancement and evolution of technologies in civil infrastructure, superlong-span cable-stayed bridges have become increasingly popular worldwide. The cable climbing robot is a typical high-altitude working mechanism, so considerable attention must be paid to its safety performance. Once a mechanical or electrical fault occurs, the robot may fall along the stay cable from a height of hundreds of meters and keep

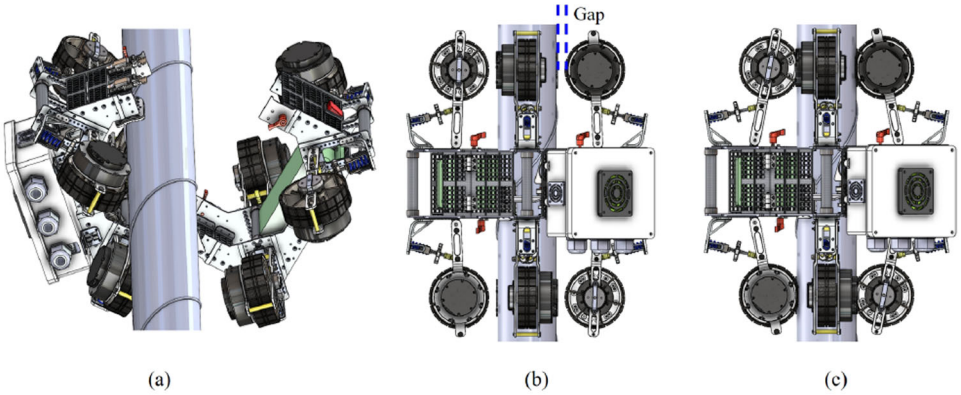

FIGURE 5 | Installation steps for the cable climbing platform, which is the shared component of the cable maintenance robot and cable rescue robot. (a) Keeping the climbing platform open. (b) Keeping the driving wheel spread out. (c) Clamping the driving wheel on the stay cable. [Color figure can be viewed at wileyonlinelibrary.com]

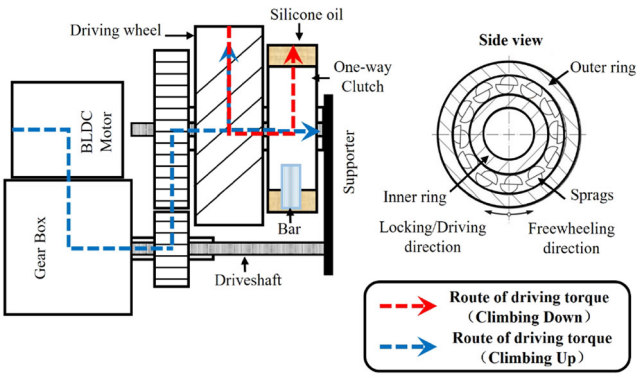

FIGURE 6 | Schematic diagram of the variable-damping safe-landing mechanism. [Color figure can be viewed at wileyonlinelibrary.com]

speeding up by its own gravity with constant acceleration until crashing on the ground, causing severe damage to the robot and potential security risks.

A novel variable-damping safe-landing mechanism is designed to enable the robot to land at a controllable velocity in case of a fault to satisfy safe landing demands. This variable-damping safe-landing mechanism structure is compact. It incorporates a one-way clutch and a silicone oil frame into the locomotion and adhesion unit, as shown in Figure 6. This unit possesses two kinds of statuses. It switches with the condition when the robot climbs up or down.

When the robot climbs up, as the blue dash-dot line shows in Figure 6, the driving wheel drives the inner ring of the one-way clutch. Since the rotating direction is freewheeling, the inner ring of the one-way clutch is independent of the outer ring of the one-way clutch. In this case, the outer ring of the one-way clutch does not rotate around the driveshaft with the one-way clutch's inner ring; the silicone oil's dampness would not affect the motion of the driving wheel.

When the robot climbs down, as the red dash-dot line shown in Figure 6, the driving wheel drives the inner ring of the one-way clutch. Since the rotating direction is locking, the outer ring of the one-way clutch rotates around the driveshaft with the inner ring of the one-way clutch simultaneously. In this case, the bar on the outer ring of the one-way clutch stirs in the silicone oil, leading to viscous damping. This damping effect could exhaust the extra energy of robot gravity and make the landing speed controllable.

It is worth noting that the viscous damping effect depends on the property of the silicone oil and the driving speed's rotating speed. In contrast to the existing safe-landing mechanism, the advantages of this solution are that the whole mechanism is compact without a fault-tolerant control system or a backup battery, and the dampness of the landing mechanism is variable in the motion process. When the climbing down speed of the climbing robot increases, viscous damping augments accordingly. This mechanism can ensure the climbing robot returns to the ground with a low velocity.

3.2 | Robotic Rescue Mechanism

Although we have designed a novel variable damp safe-landing mechanism for the climbing robot's intrinsic security, we also have to face the problem that the robot is trapped or stuck on the upper-air stay cable, which is several hundreds of meters high and can not automatically return to the ground. This study adopted an innovative solution that used a tailored cable rescue robot to drag the trapped robot back to the ground.

Figure 7 illustrates how the cable rescue robot assists the cable maintenance robot in escaping a trap. When the cable maintenance robot is trapped on the upper-air cable, a cable rescue robot is activated, and the capturing grippers should remain open, as shown in Figure 7a. Then, the cable rescue robot moves up along the stay cable. When the cable rescue robot approaches the capturing rod of the cable maintenance robot, the cable rescue robot begins to adjust the position of the capturing grippers through the circular rail to dock the capturing rod. A vision assistant system is adopted to assist docking between the capturing grippers and the capturing rod, as shown in Figure 7b. Figure 7c demonstrates that the capturing grippers close their legs and capture the capturing rod successfully. Based on that, the cable rescue robot drags the cable maintenance robot through the docking system and moves down to the

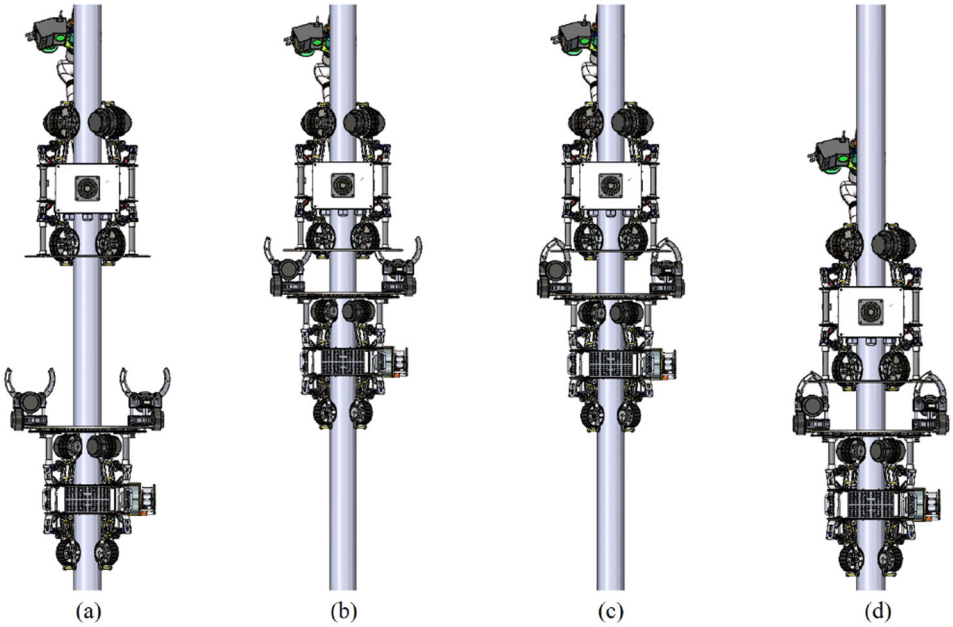

FIGURE 7 | Sequential diagram of one rescuing cycle for the robotic rescue mechanism. (a) Initial status. (b) Cable rescue robot climbs up. (c) Cable rescue robot captures the cable maintenance robot. (d) Cable rescue robot drags the cable maintenance robot down. [Color figure can be viewed at wileyonlinelibrary.com]

ground, as illustrated in Figure 7d. To this end, the robotic rescuing process is achieved.

3.3 | Fusible Gripper Mechanism

For wheel-based climbing robots, the variable-damping safe-landing mechanism and the robotic rescue mechanism developed as aforementioned are enough to deal with uncertainty factors and satisfy the requirements about the robot's intrinsic safety and robustness. Nevertheless, for palm/leg-based climbing robots (robots equipped with grippers) (Zheng et al. 2018; Zheng and Ding 2019; Ding et al. 2020; Zhang et al. 2021; Zheng et al. 2021, 2022), a more delicate matter is needed to resolve. For example, in our CCRobot series, the gripper is designed to anchor on the stay cable surface for stable status. This design may lead to challenges, such as the gripper not loosening the leg or palm clinging to the stay cable surface due to power shortages, electrical malfunctions, or mechanical breakdowns. Since there is substantial pressure between the stay cable surfaces and the palms/legs, the climbing robot can not automatically return to the ground by its gravity energy, and even a cable rescue robot can not pull down the climbing robot.

In this study, a meltable gripper is tailored for this delicate matter. As illustrated in Figure 8, a fusible alloy, which is a metal alloy capable of being fused easily at relatively low temperatures, is incorporated in the gripper, and a heating sheet clinging to the fusible alloy is installed on the gripper. A pre-loaded tension spring is applied to the palm. When the gripper could not loosen the palm by some accidents, the heating sheet would start to work, and the temperature of the fusible alloy would rise. After reaching the phase transition temperature (about 62°C), the fusible alloy begins to melt and becomes liquid. The palm anchored on the stay cable surfaces

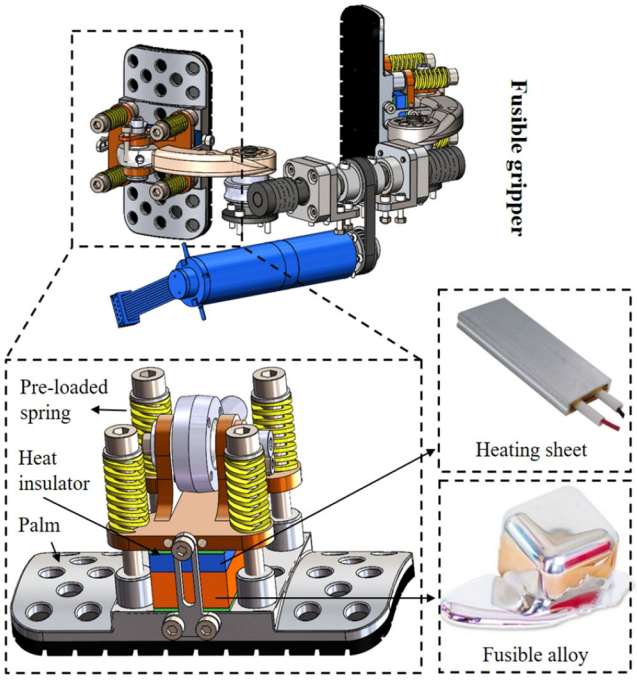

FIGURE 8 | Schematic diagram of the fusible gripper mechanism for the cable maintenance robot. [Color figure can be viewed at wileyonlinelibrary.com]

is pulled away from the stay cable surfaces by the pre-loaded tension springs. Consequently, a substantial pressure between the palms and stay cable surfaces is released, as illustrated in Figure 9. Then, the cable climbing robot can return to the ground automatically with its gravity energy, with the function of the variable damp safe-landing mechanism, or a cable rescue robot can be used to drag the cable climbing robot back to the ground.

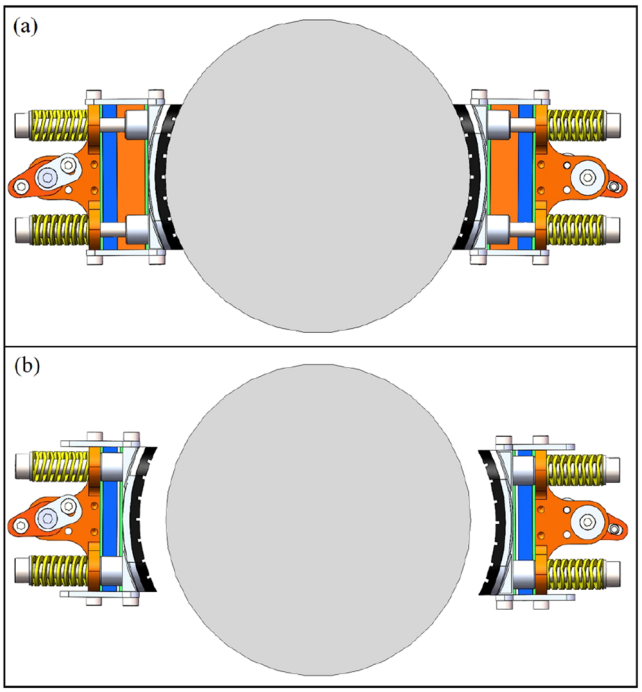

FIGURE 9 | Graphical comparisons between the positioning of the fusible gripper mechanism before and after the fusible alloy undergoes melting. (a) Before melting the fusible alloy, the palms of the gripper cling tightly to the stay cable surfaces. (b) After melting the fusible alloy, the pressure between the palms and the stay cable surfaces is released, and the palms are pulled away from the stay cable surfaces. [Color figure can be viewed at wileyonlinelibrary.com]

It needs to be highlighted that an emergency power supply system, independent of the primary power supply system, is used in the fusible gripper mechanism to provide power for the heating sheet. A remote control method is used to achieve the heating sheet's boot.

4 | Modeling and Obstacle-Negotiation Analysis

4.1 | Modeling

Both the cable maintenance robot and the cable rescue robot are based on the same climbing platform structure. In this study, we take the cable maintenance robot as an example. For the cable maintenance robot, it is a wheel-based climbing robot. Figure 10 illustrates the forces and torques acting on the cable maintenance robot. The world global coordinate frame, denoted $\{\mathcal{W}\}$, is fixed on the point of intersection between the stay cable's axis and the cable-stayed bridge deck. The body-fixed coordinate frame, denoted $\{\mathcal{B}\}$, is located on the Center of Mass (CoM) of the robot. The coordinate axes pointing of frames $\{\mathcal{W}\}$ and $\{\mathcal{B}\}$ are visualized in Figure 10. The eight driving wheels are numbered 1–8. More dynamic parameters are presented in Table 2, and we make the following assumptions:

- The robots are considered rigid bodies, and dynamic deformations are neglected.
- The wind effect is simplified as a linear variable. It is only proportional to the wind damping.

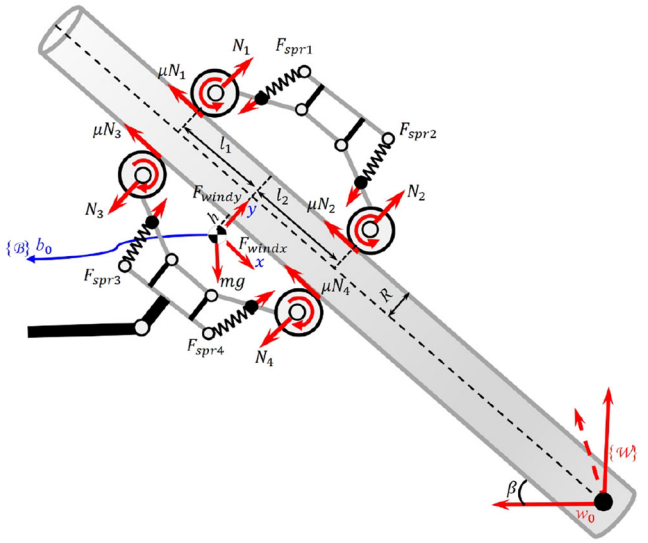

FIGURE 10 | Schematic outline of the cable maintenance robot showing the frames and forces. [Color figure can be viewed at wileyonlinelibrary.com]

TABLE 2 | Modeling parameters.

Parameters sheet			
N	Reactive force	β	Cable angle
i	Driving wheel number	m	Robot mass
g	Acceleration of gravity	μ	Friction coefficient
r	Driving wheel radius	F_{spr}	Spring force
R	Cable radius	F_{wind}	Wind resistance
D	Wind damping coefficient	h	CoM offset

- The rotation disturbance around the bridge cable of the cable climbing robot and its Euler's Equations of Motion are omitted.

$$\begin{cases} m\ddot{x} &= \mu\sum_{i=1}^{8} N_i - F_{windx} - mg\sin\beta \\ m\ddot{y} &= \sum_{i=1}^{2} N_i - \sum_{i=3}^{4} N_i + F_{windy} - mg\cos\beta \\ m\ddot{z} &= \sum_{i=5}^{6} N_i - \sum_{i=7}^{8} N_i + F_{windz} \\ \sum\tau_{b_0(p_{xy})} &= 0 = N_1 l_1 - N_2 l_2 + N_4 l_2 - N_3 l_1 \\ &\quad - \mu N_1(2R+h) - \mu N_2(2R+h) \\ &\quad - \mu N_3 h - \mu N_4 h \\ \sum\tau_{b_0(p_{xz})} &= 0 = N_5 l_1 - N_6 l_2 + N_8 l_2 - N_7 l_1 \\ &\quad - \mu N_5(2R+h) - \mu N_6(2R+h) \\ &\quad - \mu N_7 h - \mu N_8 h. \end{cases} \tag{1}$$

The force balance equations for the robot in the axial directions **x**, **y**, and **z** can be determined through the principle of mechanical equilibrium when the robot is moving forward in Equation (1),

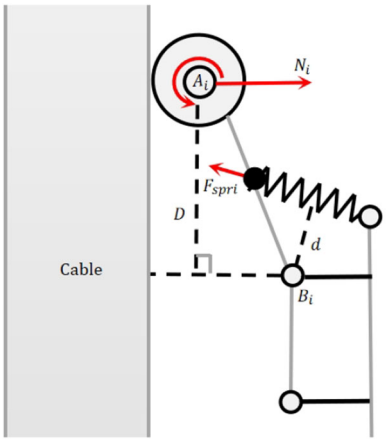

FIGURE 11 | Schematic diagram of the mechanical equilibrium for the locomotion and adhesion unit. [Color figure can be viewed at wileyonlinelibrary.com]

and the torque balance equations based on point b_0 in the plane $\mathbf{p}_{xy}$ and $\mathbf{p}_{xz}$ can also be calculated in Equation (1).

Suppose the wind damping coefficient is D, then

$$\begin{cases} F_{windx} = D_x \dot{x} \\ F_{windy} = D_y \dot{y} \\ F_{windz} = D_z \dot{z} \end{cases}. \tag{2}$$

For every locomotion and adhesion unit i as shown in Figure 11, the torque balance equation based on point B_i of the linkage A_iB_i is shown as follows:

$$N_i D - F_{spri} d = 0. \tag{3}$$

As a result, we can get the relationship between the force of the tension F_{spri} and the relative force N_i.

According to Equations (1) and (2), and because the motion of the robot is restricted in the $\mathbf{x}$ direction by the wheels and the cable, Newton's Equations of Motion can be rewritten as follows:

$$m\ddot{x} = \mu \sum_{i=1}^{8} N_i - mg \sin\beta - D_x \dot{x}, \tag{4}$$

where $N_i = \frac{F_{spri} d}{D}$ by solving Equation (3).

4.2 | Obstacle-Negotiation Analysis

The locomotion and adhesion unit incorporates a suspension mechanism, providing pre-stressing and flexible deformation capacity to overcome the obstacle. Figure 12 illustrates the obstacle-negotiation process of the driving wheel. The length of the linkage C_iB_i, A_iB_i, B_iE_i, and D_iE_i are denoted as L_1, l, L_4, and L_3, respectively. The length of the adjustable linkage C_iD_i comprised of the positive and negative screw is denoted as L. When the driving wheel surmounts the obstacle, the adjustable

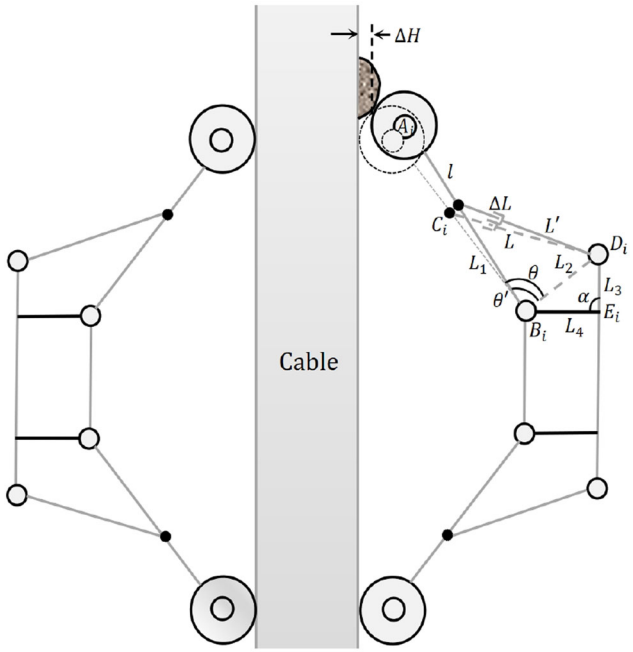

FIGURE 12 | Obstacle-negotiation analysis for the locomotion and adhesion unit.

linkage is compressed, and its length is adjusted to L', according to the cosine theorem of the triangle,

$$\begin{cases} {L_3}^2 + {L_4}^2 - 2L_3L_4\cos\alpha = {L_2}^2 \\ {L_1}^2 + {L_2}^2 - 2L_1L_2\cos\theta' = {L'}^2 \end{cases}, \tag{5}$$

we can express the relationship between the length L' and the angle θ' as shown below,

$$\theta' = \arccos\frac{{L_1}^2 + {L_3}^2 + {L_4}^2 - {L'}^2 - 2L_3L_4\cos\alpha}{2L_1\sqrt{{L_3}^2 + {L_4}^2 - 2L_3L_4\cos\alpha}}. \tag{6}$$

Meanwhile,

$$\beta = \arccos\left(\frac{{L_2}^2 + {L_4}^2 - {L_3}^2}{2L_2L_4}\right). \tag{7}$$

$$L' = L - \Delta L. \tag{8}$$

The height ΔH that the driving wheel can surmount is derived as below,

$$\Delta H = |l\cos(180° - \theta - \beta) - l\cos(180° - \theta' - \beta)|. \tag{9}$$

Substituting Equations (6), (7), and (8) into Equation (9), we can learn the relationship between the displacement ΔH and the length change of the adjustable linkage ΔL.

According to the mechanical structure of the locomotion and adhesion unit, the values of the L_1, l, L_3, L_4, and α are 66, 140, 50, 70 mm, and 99°, respectively. The initial values of L and θ are 115 mm and 91. 7°, and the adjustable length of the linkage

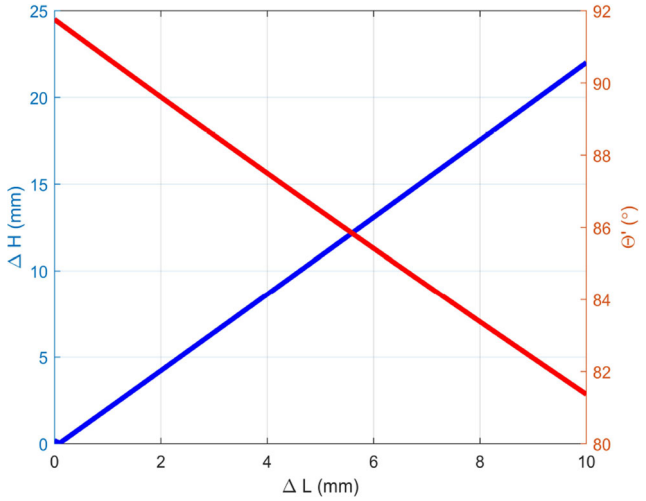

FIGURE 13 | Values variation trend of parameters ΔH and θ' when the length of the linkage C_iD_i is changing. [Color figure can be viewed at wileyonlinelibrary.com]

C_iD_i changes within the ranges of 0–10 mm. Substituting the values of the variable parameters into Equation (9), we can get the values variation trend of parameters ΔH and θ' when the length of the linkage C_iD_i is changing, as shown in Figure 13. This figure indicates that as the adjustable length of the linkage C_iD_i increases, the height of the obstacle that can be surmounted by the suspension mechanism also increases while the angle θ decreases. When the linkage C_iD_i achieves a limit adjustable length of approximately 10 mm, the theoretical maximum height of the obstacle that can be surmounted can reach approximately 22 mm.

5 | Capturing Workspace Analysis and Control

5.1 | Capturing Workspace Analysis

To determine the motion and capturing strategy of the cable rescue robot, the reachable workspace for the capturing grippers should be identified. For the cable rescue robot, the pose of the capturing gripper is our primary concern since it determines the accuracy and stability of capturing the trapped robot. To formulate the kinematics of the cable rescue robot and derive the pose of the end effector, the configuration of the cable rescue robot is established, as shown in Figure 14. We adopt a prismatic-revolute-revolute (PRR) mechanism, which is an open-type serial kinematic chain with three degrees of freedom consisting of a prismatic joint and two revolute joints to simplify the model and characterize the geometry of the mechanism by kinematic parameters.

The reference coordinate frame $\{\mathcal{W}_0\}$ is fixed on the point of intersection between the stay cable's axis and the cable-stayed bridge deck, and the coordinate frames $\{\mathcal{W}_1\}$, $\{\mathcal{W}_2\}$, and $\{\mathcal{W}_3\}$ are assigned and set up successively as the standard Denavit–Hartenberg method. In this study, we treat the locomotion of the cable rescue robot along the stay cable as the prismatic joint with the coordinate frames $\{\mathcal{W}_1\}$, the rotation of the capturing gripper is simplified as a revolute joint with the coordinate

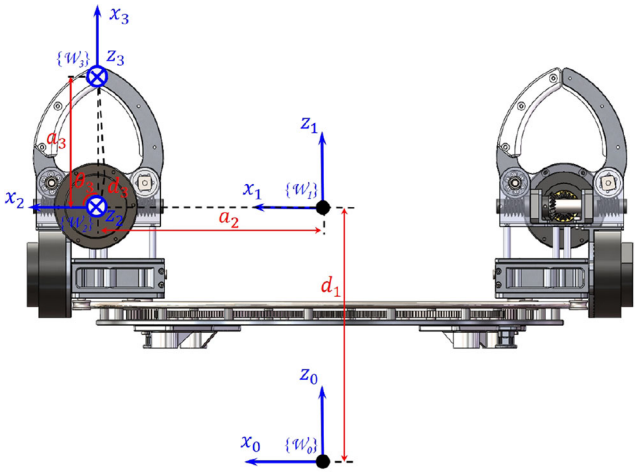

FIGURE 14 | D-H coordinate system of the capturing gripper mechanism. [Color figure can be viewed at wileyonlinelibrary.com]

TABLE 3 | Modeling parameters.

Parameters sheet					
Serial joint number i	a_i	α_i	d_i	θ_i	Joint variables
1	0	0	d_1	0	d_1
2	a_2	90°	0	θ_2	θ_2
3	a_3	0	d_3	θ_3	θ_3

frames $\{\mathcal{W}_2\}$, and the grasp motion of the capturing gripper is simplified as a revolute joint with the coordinate frames $\{\mathcal{W}_3\}$. The D–H parameters for the configuration are listed in Table 3, where a_i means the length of the link from one joint to the next along the previous link's z-axis; α_i is the angle between two consecutive z-axes, measured around the x-axis of the previous link; d_i is the offset along the previous link's z-axis from the origin of one coordinate system to the origin of the next, and θ_i is the angle between two consecutive x-axes, measured around the z-axis of the previous link.

According to the concatenating link transformations, the pose matrix of the coordinate system between adjacent linkages can be derived:

$$ {}^{0}T_1 = \begin{bmatrix} 1 & 0 & 0 & 0 \\ 0 & 1 & 0 & 0 \\ 0 & 0 & 1 & d_1 \\ 0 & 0 & 0 & 1 \end{bmatrix}. \tag{10} $$

$$ {}^{1}T_2 = \begin{bmatrix} \cos(\theta_2) & 0 & \sin(\theta_2) & a_2\cos(\theta_2) \\ \sin(\theta_2) & 0 & -\cos(\theta_2) & a_2\sin(\theta_2) \\ 0 & 1 & 0 & 0 \\ 0 & 0 & 0 & 1 \end{bmatrix}. \tag{11} $$

$$ {}^{2}T_3 = \begin{bmatrix} \cos(\theta_3) & -\sin(\theta_3) & 0 & a_3\cos(\theta_3) \\ \sin(\theta_3) & \cos(\theta_3) & 0 & a_3\sin(\theta_3) \\ 0 & 0 & 1 & d_3 \\ 0 & 0 & 0 & 1 \end{bmatrix}. \tag{12} $$

As a result, by multiplying homogeneous transformation matrices of every linkage, the homogeneous transformation matrix for the whole configuration, that is, the coordinate frame $\{\mathcal{W}_3\}$ relative to that of the coordinate frame $\{\mathcal{W}_0\}$ is deduced:

$$ {}^0T_3 = {}^0\ T_1{}^1T_2{}^2T_3 = \begin{bmatrix} n_x & s_x & a_x & p_x \\ n_y & s_y & a_y & p_y \\ n_z & s_z & a_z & p_z \\ 0 & 0 & 0 & 1 \end{bmatrix}, \tag{13} $$

where the rotation matrix for the whole configuration is as follows:

$$ \begin{aligned} {}^0R_3 &= \begin{bmatrix} n_x & s_x & a_x \\ n_y & s_y & a_y \\ n_z & s_z & a_z \end{bmatrix} \\ &= \begin{bmatrix} \cos(\theta_2)\cos(\theta_3) & -\cos(\theta_2)\sin(\theta_3) & \sin(\theta_2) \\ \cos(\theta_3)\sin(\theta_2) & -\sin(\theta_2)\sin(\theta_3) & -\cos(\theta_2) \\ \sin(\theta_3) & \cos(\theta_3) & 0 \end{bmatrix}, \end{aligned} \tag{14} $$

where the position of the end effector of the capturing gripper relative to the base coordinate system is shown as follows:

$$ \begin{aligned} p_x &= a_2\cos(\theta_2) + d_3\sin(\theta_2) + a_3\cos(\theta_2)\cos(\theta_3); \\ p_y &= a_2\sin(\theta_2) - d_3\cos(\theta_2) + a_3\cos(\theta_3)\sin(\theta_2); \\ p_z &= d_1 + a_3\sin(\theta_3). \end{aligned} \tag{15} $$

In this study, we can identify and quantify the workspace through the analytical expression Equation (15), which corresponds to the parametric equation for the admissible workspace of the capturing gripper. According to the mechanical structure of the robot, the initial values of the d_1, θ_2, and θ_3 are 0, 0°, and 0°, changing within the ranges of 0–50 mm, 0° to 360°, and 0° to 180°, respectively. Other parameters include $d_3 = 45$ mm, $a_2 = 220$ mm, and $a_3 = 115$ mm. Substituting the values of the variable parameters into this equation, we can get the working ranges of the end-effector on the **xy** plane, as shown in Figure 15. Furthermore, the operating ranges on the **x**, **y**, and **z**-axes in three-dimensional space are demonstrated in Figure 16, which shows the entire admissible workspace collecting every point that the capturing gripper can reach. We can find that the end effector of the capturing gripper operates with a length of about 200 mm, fault-tolerant for the docking process between the capturing grippers and the capturing rod.

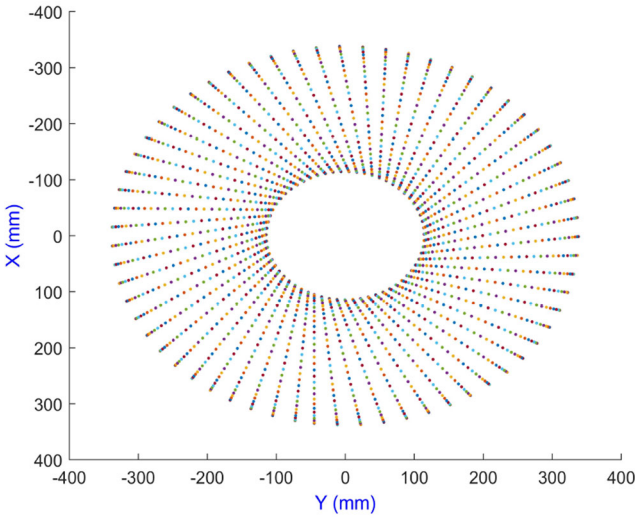

FIGURE 15 | Two-dimensional admissible workspace of the capturing gripper mechanism. [Color figure can be viewed at wileyonlinelibrary.com]

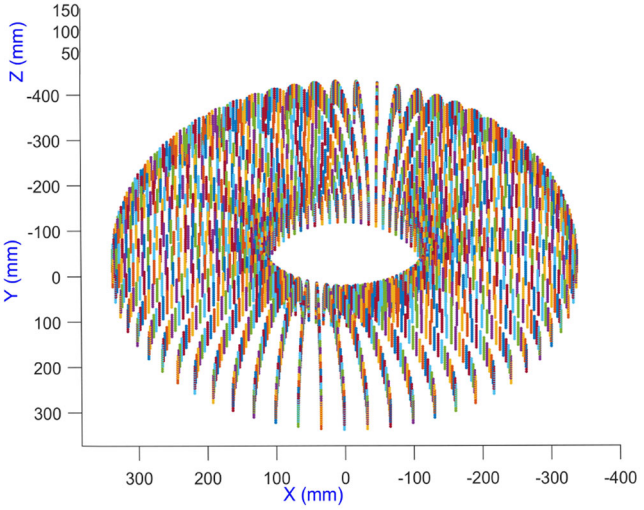

FIGURE 16 | Three-dimensional admissible workspace of the capturing gripper mechanism. [Color figure can be viewed at wileyonlinelibrary.com]

5.2 | Control System

Figure 17 shows the control architecture for the robotic system. It consists of two subsystems: a high-level and a low-level controller that communicates with each other by transmission control protocol/internet protocol (TCP/IP). The high-level controller is a ground station controller responsible for the user interface and processing of the raw data transmitted from the low-level controller. The ground station can also directly communicate with the robotic manipulator or fusible gripper. Based on a heterogeneous architecture, the low-level controller includes an onboard processor integrated into the cable maintenance or rescue robot. It is responsible for the real-time control algorithm, motion planning, and safety functions. The internal communication of the low-level controllers for the cable maintenance robot and the cable rescue robot is the Controller Area Network Open protocol (CANopen). We also develop a joystick to steer the cable maintenance and rescue robots by giving high-level commands.

6 | Experiments and Results

6.1 | Setup

Figure 18 shows the robotic system prototype, including the cable maintenance and rescue robot attached to the bridge cables. A multi-cable test platform, whose cable length spans a range from 6 to 8 m, cable diameter spans a range from 100 to 120 mm, and whose bridge tower height is about 5 m, is

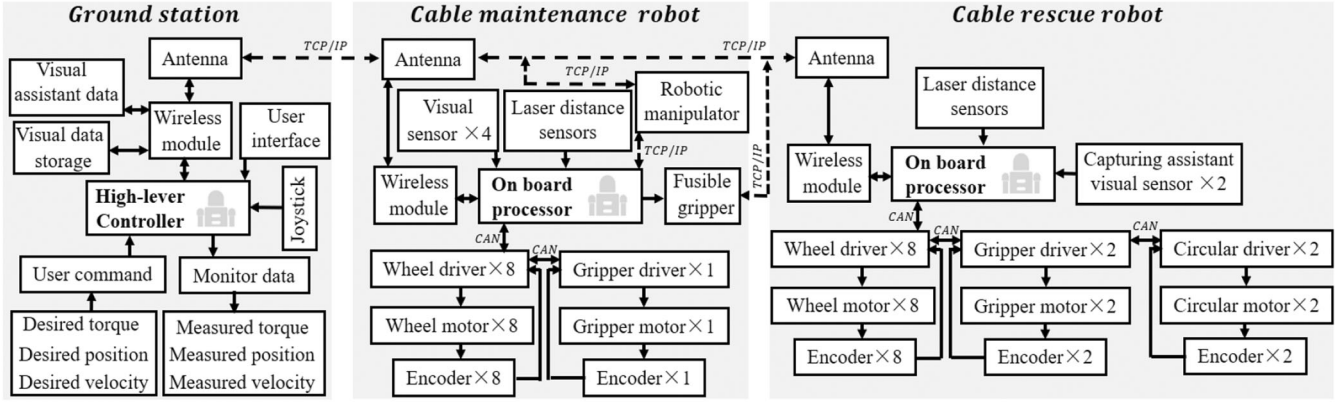

FIGURE 17 | Control system diagram for the robotic system. The control system mainly includes three parts: the ground station control system, the cable maintenance robot control system, and the cable rescue robot system. The high-level controller is equipped at the ground station, and the low-level controllers are equipped with the cable maintenance robot and cable rescue robot, respectively.

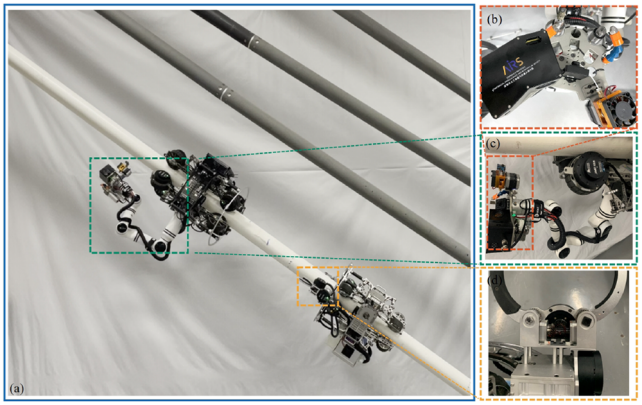

FIGURE 18 | (a) The robotic system prototype. (b) The specialized tools unit. (c) The robotic manipulator. (d) The capturing gripper. [Color figure can be viewed at wileyonlinelibrary.com]

prepared for the experiments. Two-step rings acting as bilateral obstacles with 10 and 20 mm heights (unilateral heights: 5 and 10 mm), which can be observed in the attached video clips, were set on the cable surface, respectively. Meanwhile, two 15 kg load weights were prepared for the load capacity test of the cable climbing robot. In this section, we first tested the capacity of the cable climbing robots, including the field test, the Payload & the obstacle-negotiation capacity test, and the maintenance capacity tests. Then, the security and rescue mechanisms were tested, including the variable-damping safe-landing mechanism test, the robotic rescue mechanism test, and the fusible gripper mechanism test. The performance and capabilities of the robotic system were extensively validated and successfully tested on the multi-cable replica, demonstrating its superiority in payload, intrinsic safety, and robustness. The specifications are summarized in Table 4.

TABLE 4 | Specifications of the robotic system.

Parameters	Values
Cable maintenance robot weight	≈ 25 kg
Cable rescue robot weight	≈ 15 kg
Climbing platform weight	9 kg
Specialized tools unit weight	4.5 kg
Robotic manipulator weight	7.8 kg
Cable diameter for climbing	90–120 mm
Battery capacity	24 V 20 AH
Dimension of CRR	43.5 × 43.5 × 60 cm
Dimension of CMR (without RM and ST)	43.5 × 43.5 × 55 cm
Climbing platform dynamic payload	45 kg
Maximum climbing speed of climbing platform	1 m/s
Maximum climbing angle	90°
Maximum height of obstacle-crossing for CMR	10 mm

Abbreviations: CMR, cable maintenance robot; CRR, cable rescue robot; RM, robotic manipulator; ST, specialized tools.

6.2 | Cable Climbing Robots Test

6.2.1 | Field Test of the Climbing Platform

Both the cable maintenance robot and the cable rescue robot are based on the same climbing platform. It is vital to assess the motion performance and validate the climbing platform in the field condition. We conducted tests on a dozen cable-stayed bridges, including the Lijiatuo Yangtze River Bridge, Xisha Bridge, Wuling Mountain Bridge, Masangxi Yangtze River Bridge, Dafosi Yangtze River Bridge, and so on, as shown in Figure 19. The climbing platform has been tested on more than 500 stay cables, with an accumulative trip of approximately half a million meters. In the testing process, various harsh conditions were experienced, such as the moss-covered cable surface, helical rib obstacle-covered cable surface, and high temperature and humid environment. Consequently, the test tasks were completed successfully on the stay cables. This test demonstrates the climbing platform's powerful motion ability and realistic deployment capacity.

FIGURE 19 | Field test and realistic deployment of the climbing platform, which has been tested on more than 500 stay cables, with an accumulative trip of approximately half a million meters. [Color figure can be viewed at wileyonlinelibrary.com]

6.2.2 | Payload and Obstacle-Negotiation Capacity Test

It is vital to evaluate the payload and obstacle-negotiation capacity of the cable climbing robots.

- In the experiments, we applied a 30 kg load weight and approximately 15 kg maintenance devices (a robotic manipulator and a specialized tool unit) on the climbing platform and let it climb along a stay cable, whose inclination angle is approximately 45°.
- A series of obstacle-negotiation capacity tests were conducted with the climbing platform on the stay cable. Bilateral step obstacles with 10 and 20 mm heights (unilateral heights: 5 and 10 mm) were set on the cable surface. The experimental results indicate that the climbing platform travels smoothly along the stay cable under these conditions.

As a result, the climbing platform endows the cable maintenance robot and the cable rescue robot with heavy-duty capacity and obstacle-negotiation ability.

6.2.3 | Maintenance Capacity Tests

To assess the maintenance capacity of the cable maintenance robot, we conducted experiments on the stay cable. When the climbing platform is integrated with four high-definition cameras installed 90° apart circumferentially, the cable maintenance robot can detect imperfections in the entire cable surface. Figure 20 shows the real imperfections on the stay cables in the field tests captured by the camera sensors on the cable maintenance robot. The cable maintenance robot can perform cable repair or grinding tasks when the climbing platform is integrated with seven DoF robotic manipulators and specialized tools.

FIGURE 20 | Imperfections of the cable surfaces captured by the high-definition camera sensors. [Color figure can be viewed at wileyonlinelibrary.com]

6.3 | Security and Rescue Mechanisms Test

6.3.1 | Damper Calibration for Variable-Damping Wheel Unit

To better analyze the landing process of the cable climbing robot once a mechanical or an electrical fault occurs, the resistance torque calibration experiments for the one-way variable-damping wheel unit were conducted to characterize the resistance torque of the damper under different rotating

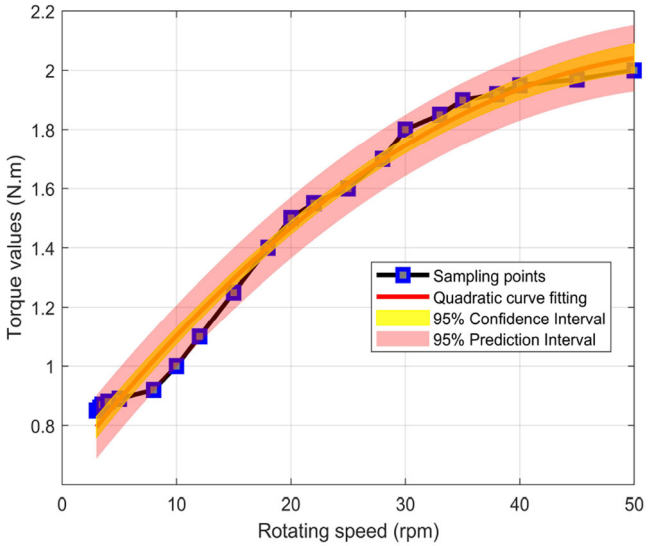

FIGURE 21 | The variable-damping characteristic under different rotating speeds of the driving wheel. [Color figure can be viewed at wileyonlinelibrary.com]

speeds of the variable-damping wheel. A servo motor is integrated into the variable-damping wheel unit. Serial rotating speeds along the locking/driving direction, as shown in Figure 6, were given to the servo motor by the motor controller; meanwhile, the servo motor's applied stable currents/torques were recorded. The results of repeated tests, as shown in Figure 21, indicated that the resistance torque of the variable-damping wheel unit is variable; it increases, as does the rotating speed of the servo motor. A quadratic fitting curve through the sampling data points was performed to estimate the damping of the variable-damping wheel unit according to the rotating speed of the variable-damping wheel. The prediction ranges of the actual values were also investigated and illustrated in Figure 21 at a 95% confidence interval level and a 95% prediction interval level regarding the fitting curve, respectively.

6.3.2 | Variable-Damping Safe-Landing Mechanism Test

We conducted tests to validate the effects of the variable-damping safe-landing mechanism. When the robot climbed up along the stay cable and approached the top of the stay cable, the power supply was suspended. The performance of the robot climbing down along the stay cable depended on whether the variable-damping safe-landing mechanism is integrated into the locomotion and adhesion unit for two cases as follows:

- Without the variable-damping safe-landing mechanism: the robot was driven by the weight of the robot. Since the low gear reduction ratio of 6 of the adopted gearbox, the robot could move towards the ground along the stay cable by its gravity with low gear resistance from the gearbox of the driving motor. As a result, the robot kept speeding up to almost 1 m/s and crashed on the ground at this high speed due to the potential energy when the power supply was deactivated. Figure 22 recorded the climbing speed and position variation over time for the climbing robot.
- With the variable-damping safe-landing mechanism: the robot can move toward the ground along the stay cable by the potential energy; however, under the function of the variable-damping safe-landing mechanism, the robot could climb down with an almost constant low speed and reach the ground safely. The variation of position and velocity over time for the climbing robot is studied and analyzed in Figure 22.

Compared to the velocity and position curves of the robot falling with and without the variable-damping safe-landing mechanism as shown in Figure 22, we can see the functions of the variable-damping safe-landing mechanism in the climbing robot's landing process. The variable-damping safe-landing mechanism can promise safety when the climbing robot encounters uncertainty factors.

6.3.3 | Robotic Rescue Mechanism Test

In this part, the robotic rescue mechanism was illustrated by the experiment. A cable maintenance robot was trapped on the top of the stay cable and could not climb down by itself. Then, a cable rescue robot was installed on the cable and moved towards the trapped robot. When the cable rescue robot approached the trapped robot, it adjusted the position of the capturing grippers and grasped the trapped robot's capturing rod. To this end, the rescue robot would drag the trapped robot back to the ground. This experiment verified the feasibility and effectiveness of the robotic rescue mechanism. Figure 23 shows the action sequence of the rescue process, and the entire robotic rescue process can be observed in the attached video clips.

6.3.4 | Fusible Gripper Mechanism Test

In this part, the fusible gripper mechanism was illustrated by the experiment. A cable maintenance robot was trapped on the stay cable since the gripper was clamped on the stay cable and could not be released due to power shortages, electrical malfunctions, or mechanical breakdowns. In this case, we activated the heating sheet through TCP/IP on the ground, and the fusible alloy was melted. Consequently, substantial pressure was released between the palm and stay cable surfaces. Then, the cable climbing robot returned to the ground automatically with its gravity energy. This experiment verified the feasibility and effectiveness of the fusible gripper mechanism.

7 | Conclusions and Future Works

This paper introduces a novel climbing robot for stay cable maintenance, possessing heavy payload characteristics of 45 kg and an obstacle-negotiation capacity of 10 mm. Several security and rescue mechanisms, including the variable-damping safe-landing mechanism, robotic rescue mechanism, and fusible gripper mechanism, were developed to deal with uncertainty factors or counteract more substantial disturbances in worse-case environments; under the functions of the variable-damping safe-landing mechanism, the maximum falling speed can decrease from 1 to 0.1 m/s to promise safety, and the falling time can increase from about 5 to 45 s. The prototype of the

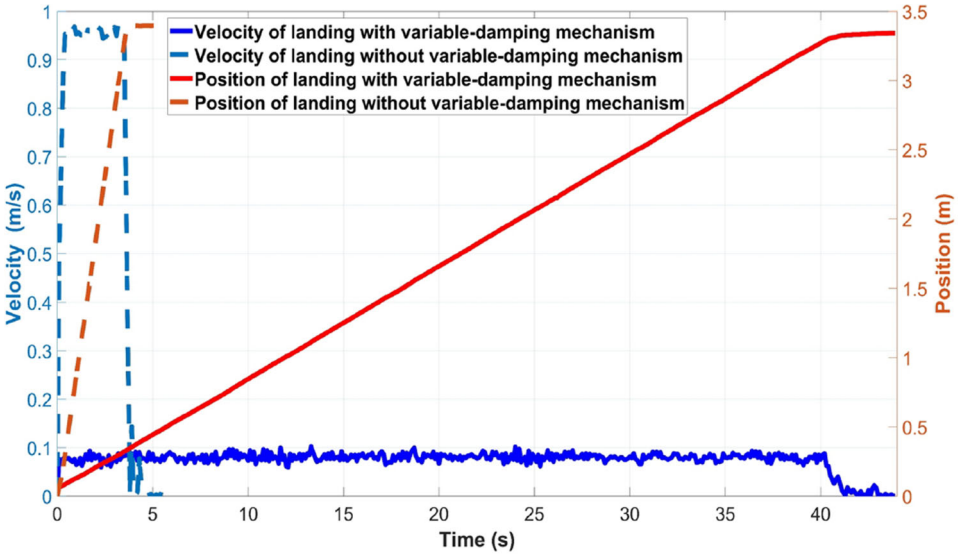

FIGURE 22 | Velocity and position curves of the robot falling with and without the variable-damping safe-landing mechanism. Under the functions of the variable-damping safe-landing mechanism, the maximum falling speed can decrease from 1 to 0.1 m/s to promise safety, and the falling time can increase from about 5 to 45 s. [Color figure can be viewed at wileyonlinelibrary.com]

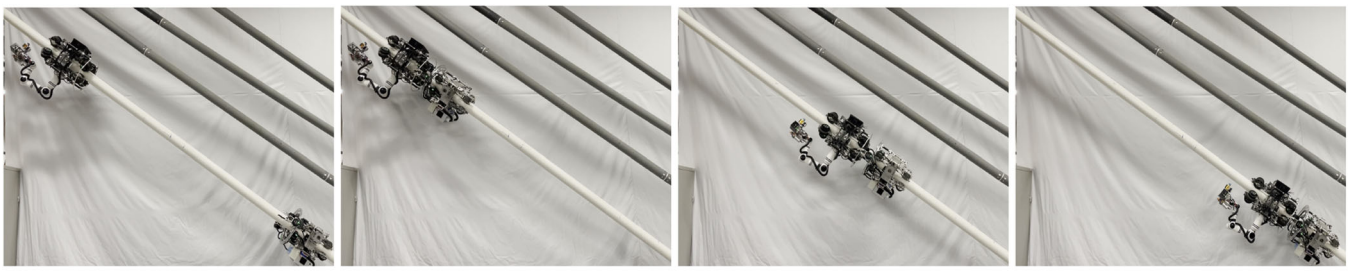

(a) Initial position (b) Cable rescue robot climbs up (c) Drag the maintenance robot down (d) One rescuing cycle ends

FIGURE 23 | Action sequence of the rescue process presents how a cable rescue robot rescues a cable maintenance robot trapped on the upper-air stay cable.

climbing robotic system has been designed and validated through various experiments. The contribution of this study can be summarized as follows:

- This study designs a novel robotic system combining heavy-duty capacity, intrinsic safety, and robustness, advancing state-of-the-art climbing technology.
- The robotic design, including security and rescue mechanisms, promotes practical applications for stay cable maintenance, closing the gap between the laboratory and realistic deployable robots.
- The proposed methodology establishes an innovative climbing and retrieving paradigm for scenarios with challenging gravity-adversarial conditions, opening the opportunity and paving the way for developing high-quality climbing robots. Researchers can leverage this approach as a foundation for designing climbing and retrieving systems in diverse applications.

Our next phase involves integrating more perceptual sensors to achieve fully autonomous climbing, maintenance, and retrieving. Additionally, we will optimize the mechanism and further improve the system performance and robustness to facilitate the realistic deployment of the robotic system in the actual bridge cable maintenance tasks.

Acknowledgments

This study was funded by Shenzhen Science and Technology Innovation Council (grant GJHZ20240218114202004), Shenzhen Science and Technology Program (grants 20220817171811004, JSGG20210802152801004), the National Natural Science Foundation of China (grant 62106155), the Guangdong Basic and Applied Basic Research Foundation (grants 2023A1515012570, 2021B1515420005), the Shenzhen Major Science Technology Project (grant KJZD20230923114810022), and the Longgang District Shenzhen's "Ten Action Plan" for Supporting Innovation Projects (grant LGKCSDPT2024002).

Data Availability Statement

Data that support the findings of this study are available on request from the corresponding author. The data are not publicly available due to privacy or ethical restrictions.

References

Backus, S. B., R. Onishi, A. Bocklund, A. Berg, E. D. Contreras, and A. Parness. 2020. "Design and Testing of the Jpl-Nautilus Gripper for Deep-Ocean Geological Sampling." *Journal of Field Robotics* 37, no. 6: 972–986.

Cho, K. H., Y. H. Jin, H. M. Kim, and H. R. Choi. 2014. "Development of Novel Multifunctional Robotic Crawler for Inspection of Hanger Cables in Suspension bridges." In *2014 IEEE International Conference on Robotics and Automation (ICRA)*, 2673–2678. IEEE.

Cho, K. H., Y. H. Jin, H. M. Kim, H. Moon, J. C. Koo, and H. R. Choi. 2013. "Caterpillar-Based Cable Climbing Robot for Inspection of Suspension Bridge Hanger Rope." In *2013 IEEE International Conference on Automation Science and Engineering (CASE)*, 1059–1062. IEEE.

Cho, K. H., Y. H. Jin, H. M. Kim, H. Moon, J. C. Koo, and H. R. Choi. 2016. "Multifunctional Robotic Crawler for Inspection of Suspension Bridge Hanger Cables: Mechanism Design and Performance Validation." *IEEE/ASME Transactions on Mechatronics* 22, no. 1: 236–246.

Cho, K. H., H. M. Kim, Y. H. Jin, et al. 2013. "Inspection Robot for Hanger Cable of Suspension Bridge: Mechanism Design and Analysis." *IEEE/ASME Transactions on Mechatronics* 18, no. 6: 1665–1674.

Ding, N., Z. Zheng, J. Song, Z. Sun, T. L. Lam, and H. Qian. 2020. "Ccrobot-iii: A Split-Type Wire-Driven Cable Climbing Robot for Cable-Stayed Bridge Inspection." In *2020 IEEE International Conference on Robotics and Automation (ICRA)*, 9308–9314. IEEE.

Hong, S., Y. Um, J. Park, and H.-W. Park. 2022. "Agile and Versatile Climbing on Ferromagnetic Surfaces With a Quadrupedal Robot." *Science Robotics* 7, no. 73: eadd1017.

IPC. 2015. *Cablescan®Cable Stayed Bridge Inspection Service*. https://www.infrastructurepc.com/cablescan/.

Lam, T. L., and Y. Xu. 2011. "Climbing Strategy for a Flexible Tree Climbing Robot Treebot." *IEEE Transactions on Robotics* 27, no. 6: 1107–1117.

Lam, T. L., and Y. Xu. 2012a. "Biologically Inspired Tree-Climbing Robot With Continuum Maneuvering Mechanism." *Journal of Field Robotics* 29, no. 6: 843–860.

Lam, T. L., and Y. Xu. 2013. "Motion Planning for Tree Climbing With Inchworm-Like Robots." *Journal of Field Robotics* 30, no. 1: 87–101.

Lam, T. L., and Y. S. Xu. 2012b. *Tree Climbing Robot: Design, Kinematics and Motion Planning*. Springer.

Li, J., X. Liu, S. Jiang, R. Li, and L. Ren. 2009. "Design of Continuous Climbing Pneumatic Cable Maintenance Robot." In *Mechatronics and Automation, 2009. ICMA 2009. International Conference on*, 4633–4637. IEEE.

Luo, J., S. Xie, Z. Gong, and T. Lu. 2007. "Development of Cable Maintenance Robot for Cable-Stayed Bridges." *Industrial Robot: An International Journal* 34, no. 4: 303–309.

Nguyen, S. T., K. T. La, and H. M. La. 2024. "Agile Robotic Inspection of Steel Structures: A Bicycle-Like Approach With Multisensor Integration." *Journal of Field Robotics* 41, no. 2: 396–419.

Nguyen, S. T., H. Nguyen, S. T. Bui, T. D. Ngo, H. M. La, et al. 2022. "An Agile Bicycle-Like Robot for Complex Steel Structure Inspection." In *2022 International Conference on Robotics and Automation (ICRA)*, 157–163. IEEE.

Parness, A., M. Frost, N. Thatte, et al. 2013. "Gravity-Independent Rock-Climbing Robot and a Sample Acquisition Tool With Microspine Grippers." *Journal of Field Robotics* 30, no. 6: 897–915.

Sika. 2021. *Solutions for Bridges and Highways*. https://mys.sika.com/en/solutions-forprojects/bridges.html.

Spenko, M., G. C. Haynes, J. Saunders, et al. 2008. "Biologically Inspired Climbing With a Hexapedal Robot." *Journal of Field Robotics* 25, no. 4–5: 223–242.

Tavakoli, M., G. Cabrita, R. Faria, L. Marques, and A. T. de Almeida. 2012. "Cooperative Multi-Agent Mapping of Three-Dimensional Structures for Pipeline Inspection Applications." *International Journal of Robotics Research* 31, no. 12: 1489–1503.

Tavakoli, M., L. Marques, et al. 2011. "3DCLIMBER: Climbing and Manipulation Over 3D Structures." *Mechatronics* 21, no. 1: 48–62.

Wang, Z., B. He, Y. Zhou, K. Liu, and C. Zhang. 2021. "Design and Implementation of a Cable Inspection Robot for Cable-Stayed Bridges." *Robotica* 39, no. 8: 1417–1433.

Xu, F., S. Dai, Q. Jiang, and X. Wang. 2021. "Developing a Climbing Robot for Repairing Cables of Cable-Stayed Bridges." *Automation in Construction* 129: 103807.

Xu, F., J. Hu, and G. Jiang. 2015. "The Obstacle-Negotiation Capability of Rod-Climbing Robots and the Improved Mechanism Design." *Journal of Mechanical Science and Technology* 29, no. 7: 2975–2986.

Xu, F., J. L. Hu, X. Wang, and G. Jiang. 2014. "Helix Cable-Detecting Robot for Cable-Stayed Bridge: Design and Analysis." *International Journal of Robotics and Automation* 29, no. 4: 406–414.

Xu, F., X. Wang, and P. Cao. 2011. "Design and Application of a New Wheel-Based Cable Inspection Robot." In *2011 IEEE International Conference on Robotics and Automation (ICRA)*, 4909–4914. IEEE.

Xu, F., X. Wang, and L. Wang. 2011. "Cable Inspection Robot for Cable-Stayed Bridges: Design, Analysis, and Application." *Journal of Field Robotics* 28, no. 3: 441–459.

Yuan, J., X. Wu, Y. Kang, and A. Ben. 2010. "Research on Reconfigurable Robot Technology for Cable Maintenance of Cable-Stayed Bridges In-Service." In *2010 International Conference on Mechanic Automation and Control Engineering*, 1019–1022. IEEE.

Zhang, W., Z. Zheng, X. Fu, et al. 2021. "Ccrobot-iv-f: A Ducted-Fan-Driven Flying-Type Bridge-Stay-Cable Climbing Robot." In *2021 IEEE/RSJ International Conference on Intelligent Robots and Systems (IROS)*, 4184–4190. IEEE.

Zheng, Z., and N. Ding. 2019. "Design and Implementation of Ccrobot-ii: A Palm-Based Cable Climbing Robot for Cable-Stayed Bridge Inspection." In *2019 International Conference on Robotics and Automation (ICRA)*, 9747–9753. IEEE.

Zheng, Z., N. Ding, H. Chen, et al. 2022. "Ccrobot-v: A Silkworm-Like Cooperative Cable-Climbing Robotic System for Cable Inspection and Maintenance." In *2022 International Conference on Robotics and Automation (ICRA)*, 164–170. IEEE.

Zheng, Z., S. Hu, and N. Ding. 2018. "A Biologically Inspired Cable Climbing Robot: Ccrobot-Design and Implementation." In *2018 IEEE International Conference on Robotics and Biomimetics (ROBIO)*, 2354–2359. IEEE.

Zheng, Z., W. Zhang, X. Fu, et al. 2021. "Ccrobot-iv: An Obstacle-Free Split-Type Quad-Ducted Propeller-Driven Bridge Stay Cable-Climbing Robot." *IEEE Robotics and Automation Letters* 7, no. 4: 11751–11758.

Supporting Information

Additional supporting information can be found online in the Supporting Information section.